# Minimum switching limit cycle oscillations for systems of coupled double integrators

Andrea Garulli, Antonio Giannitrapani, Mirko Leomanni

*Abstract*— **In this paper, we study the limit cycle oscillations of multiple double integrators with coupled dynamics, subject to a constant disturbance term and switching inputs. Such systems arise in a variety of control problems where the minimization of both fuel and number of input transitions is a key requirement. The problem of finding the minimum switching limit cycle, among all the fuel-optimal solutions satisfying given state constraints, is addressed. Starting from well known results available for a single double integrator, two suboptimal solutions are provided for the multivariable case. First, an analytic upper bound on the number of input switchings is derived. Then, a less conservative numerical solution exploiting the additional degrees of freedom provided by the phases of the limit cycles is presented. The proposed techniques are compared on two simulation examples.**

## I. Introduction

Relay feedback systems are a classic topic in control theory (see e.g. [1], [2], [3] and references therein). It is well known that a large class of relay feedback systems presents limit cycle oscillations and a huge number of results are available in the literature concerning existence and stability conditions for such limit cycles. However, most of the literature deals with single-input single-output systems, while relatively few results are available for the multivariable case [4], [5], [6].

In recent years, a significant effort has been devoted to the study of limit cycles in more general classes of systems, such as piecewise affine systems or hybrid systems [7], [8], [9]. For many practical applications, limit cycles are indeed a feasible solution, but it is required to keep the number of input transitions as low as possible, due to technological limitations or to the need of maximising the lifetime of the actuators. Consequently, the performance objective is often modified in order to penalise in some way the number of input transitions, which in turn affect the switching among the modes of the system. Applications of such problems can be found in power electronics [10], air conditioning systems [11], boiler control systems [12], attitude control [13].

Explicit solutions to minimum switching control problems with state constraints have been derived only for very simple systems. One notable example, that is indeed useful in many applications, is the double integrator subject to a constant forcing term. This system has been studied in detail, for instance, for the single-axis attitude control problem with on/off actuators, and the limit cycle corresponding to the fuel/switch-optimal steady state solution has been fully characterised [14], [15]. More recently, this case study has been thoroughly analysed in the context of event-based control [16].

The aim of this paper is to address a minimum switching control problem for a multivariable system consisting of $n$ coupled double integrators, subject to a constant forcing term and controlled by $n$ switching actuators. One of the motivating applications is a multi-axis attitude control problem in which non orthogonal thruster configurations are adopted, in order to maximize the generated torque or to satisfy constraints deriving from the spacecraft layout. In this context, the minimisation of the frequency of thruster firings is a key requirement, especially when electric thrusters are employed for attitude control [13]. The contribution of the paper is twofold. First, an analytic upper bound to the minimum number of switchings is derived, by suitably extending the single-axis results of [14], [15] to the multivariable case. Since the corresponding solution does not depend on the relative phases of the single-axis trajectories, a less conservative solution is found numerically by exploiting these further degrees of freedom. The benefits of the latter approach are demonstrated by means of two simulation examples.

The paper is organized as follows. Section II introduces the minimum fuel and minimum switching control problems for a single-axis double integrator, and briefly reviews the solution of such problems. Then, Section III addresses the multivariable problem, for a system of coupled double integrators, and provides the main results of the paper. The numerical examples are presented in Section IV, while some concluding remarks are given in Section V.

## II. Single-axis problem formulation

Consider the forced double integrator

$$\begin{aligned} \dot{x}_1(t) &= x_2(t) \\ \dot{x}_2(t) &= u(t) + k\,, \end{aligned} \tag{1}$$

where

$$u(t) \in \{-1,\, 0,\, 1\} \tag{2}$$

and $k \neq 0$ is a known constant forcing term, such that $|k| < 1$ to ensure controllability of the system. The objective of the control system is to guarantee that

$$|x_1(t)| \leq \delta, \tag{3}$$

The authors are with the Dipartimento di Ingegneria dell'Informazione e Scienze Matematiche, Università di Siena, Siena, Italy. Email: {garulli,giannitrapani,leomanni}@dii.unisi.it.

where $\delta$ is a known bound. Then, the fuel-optimal control problem can be formulated as

$$\begin{array}{ll} \min\limits_{u} & J_f(u) = \lim\limits_{T\to\infty} \dfrac{1}{T}\displaystyle\int_0^T |u(t)|\,dt \\ \text{s.t.} & (1), (2), (3). \end{array} \tag{4}$$

The following proposition is a standard result from optimal control theory.

*Proposition 1:* A necessary condition for $u^*(t)$ to be a solution to problem (4) is

$$u^*(t) \in \{0,\, -\bar{k}\}, \tag{5}$$

where $\bar{k} = \text{sgn}(k)$. Moreover,

$$J_f(u^*) = |k|. \tag{6}$$

*Proof:* By (1)-(3), $x_2(t)$ is bounded. Then

$$\lim_{T\to\infty} \frac{1}{T}\left(x_2(0) + \int_0^T (u(t)+k)\,dt\right) = 0,$$

which gives

$$\lim_{T\to\infty} \frac{1}{T}\int_0^T u(t)\,dt = -k. \tag{7}$$

Hence, the solution to (4) is also a minimizer of problem

$$\begin{array}{ll} \min\limits_{u} & J_f(u) \\ \text{s.t.} & (2), (7). \end{array} \tag{8}$$

It is straightforward to check that $u(t) \in \{0,\, -\bar{k}\}$ is a necessary condition for the optimal solution of (8). By enforcing this condition in (7), it follows that $J_f(u) = |k|$. ■

Among all the fuel-optimal input sequences satisfying (3), we aim at finding the one which minimizes the average number of input transitions, i.e. the one solving the problem

$$\begin{array}{ll} \min\limits_{u} & J_s(u) = \lim\limits_{T\to\infty} \dfrac{1}{T}\displaystyle\int_0^T |\dot{u}(t)|\,dt \\ \text{s.t.} & (1), (3), (5). \end{array} \tag{9}$$

The solution to (9) can be found by using phase plane arguments, as described next. According to (5), $u(t) \in \{0,\, -\bar{k}\}$. The trajectories obtained for $u(t) = 0$ and $u(t) = -\bar{k}$ in (1) are reported in the phase plane in Fig. 1, where it has been assumed $\bar{k} = 1$ (the reasoning is analogous for $\bar{k} = -1$). From (3) and (5), it follows that fuel-optimal state trajectories are bounded paths switching between the curves in Fig. 1, which differ in amplitude and number of input transitions.

Let

$$\psi^u = \{(x_1, x_2) :\ \bar{k}x_1 = \tfrac{1}{2(|k|-1)}\, x_2^2 + \delta,\ \ \bar{x}_1 \le \bar{k}x_1 \le \delta\}$$
$$\psi^k = \{(x_1, x_2) :\ \bar{k}x_1 = \tfrac{1}{2|k|}\, x_2^2 - \delta,\ \ -\delta \le \bar{k}x_1 \le \bar{x}_1\},$$

where $\bar{x}_1 = \delta(1-2|k|)$. Then, the following result characterizes the unique fuel-optimal solution that is also switch-optimal [14], [15].

*Proposition 2:* The fuel/switch-optimal solution to (9) is

$$u^*(t) = \begin{cases} -\bar{k} & \text{if} \quad (x_1(t),\, x_2(t)) \in \psi^u \\ 0 & \text{if} \quad (x_1(t),\, x_2(t)) \in \psi^k \end{cases} \tag{10}$$

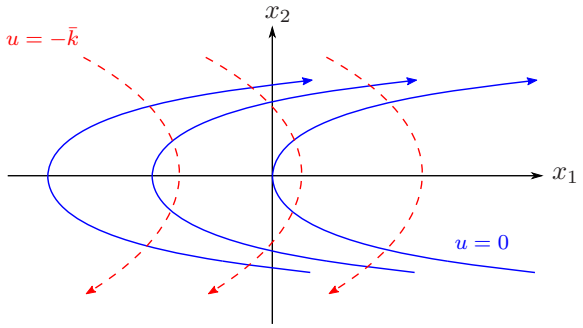


Fig. 1. Trajectories of (1) for $u = 0$ (solid) and $u = -\bar{k}$ (dashed).

*Proof:* It follows by integration of system (1) with either $u = 0$ or $u = -\bar{k}$ and by taking the solution which maximizes the time between two consecutive input transitions, while satisfying constraint (3). ■

Fig. 2 shows the fuel/switch-optimal solution provided by Proposition 2, for $\bar{k} = \text{sgn}(k) = 1$. The trajectory of system (1) along the double-switch periodic limit cycle $\psi^u \cup \psi^k$ can be expressed as

$$\begin{array}{rcl} x_1(t) & = & a\, f(t/p + \phi) \\ x_2(t) & = & \dot{x}_1(t) \\ a & = & p^2\,\gamma \\ \gamma & = & |k|\,(1-|k|)/16, \end{array} \tag{11}$$

where $a = \delta$ is the amplitude, $p$ is the period, $\phi \in [0, 1]$ is the phase of the limit cycle, and $f(\xi)$ is a periodic function given by

$$f(\xi) = \begin{cases} \bar{k}\left(1 - \frac{8}{|k|}\,(\lambda - \frac{|k|}{2})^2\right) & 0 \le \lambda \le |k| \\ -\bar{k}\left(1 + \frac{8}{|k|-1}(\lambda - \frac{|k|+1}{2})^2\right) & |k| \le \lambda \le 1 \end{cases}$$
$$\lambda \ = \ \text{mod}\,(\xi, 1). \tag{12}$$

From (10) and (11), it follows that the optimal input signal $u^*(t)$ is pulse-width modulated with period $p^* = \sqrt{\delta/\gamma}$ and duty cycle $|k|$.

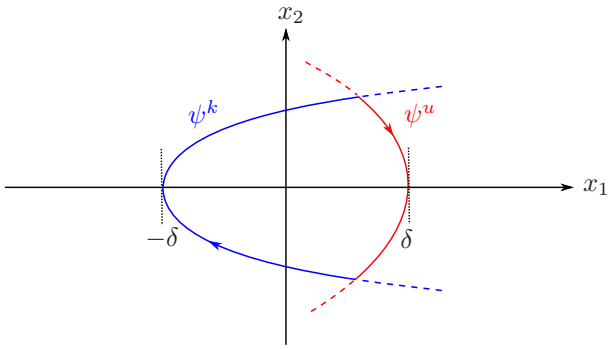


Fig. 2. Fuel/switch-optimal solution to problem (9).

Notice that Proposition 2 provides a minimum switching and fuel-optimal trajectory for system (1), under the constraint (2) and (3), in terms of a limit cycle in the phase plane. In order to steer the system state to this limit cycle

from any initial condition, the following control law can be employed

$$u(t) = \begin{cases} -\bar{k} & \text{if} \quad (x_1(t),\, x_2(t)) \in R_1 \cup \varphi^u \\ 0 & \text{if} \quad (x_1(t),\, x_2(t)) \in R_2 \cup \varphi^k \end{cases}$$

where $R_1$ and $R_2$ are the open portions of the phase plane separated by the curves $\varphi^u$ and $\varphi^k$, shown in Fig. 3 for the case $\bar{k} = 1$.

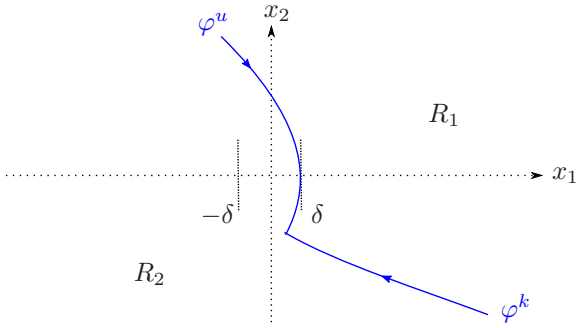


Fig. 3. Fuel/switch-optimal switching curve.

## III. Coupled double integrators

The aim of this paper is to generalize the results in Section II to the multivariable system defined by

$$\dot{x} = Ax + Bu + B_d d, \tag{13}$$

where

$$A = \begin{bmatrix} 0 & I \\ 0 & 0 \end{bmatrix}, \qquad B = \begin{bmatrix} 0 \\ B_v \end{bmatrix}, \qquad B_d = \begin{bmatrix} 0 \\ I \end{bmatrix},$$

$x = [x_r^T,\, x_v^T]^T$, $x_r,\, x_v \in \mathbb{R}^n$, $u \in \{-1,\, 0,\, 1\}^n$, $d \in \mathbb{R}^n$ and $\|B_v^{-1}\, d\|_\infty < 1$. These equations describe a system of $n$ double integrators, controlled by $n$ switching inputs, which are coupled through the $n \times n$ matrix $B_v$. In this case, the constraint (3) can be generalized to

$$\|W\, x_r(t)\|_\infty \leq 1, \tag{14}$$

where $W = \text{diag}(\delta_1, \ldots, \delta_n)^{-1}$. If $B_v$ is diagonal, the double integrators in (13) are decoupled and the results of Section II can be applied separately to each input channel. The nontrivial case in which $B_v$ is not diagonal is addressed next.

Under the assumption that $B_v$ is full-rank, we define the new state variables $y = T^{-1}x$, with

$$T = \text{blockdiag}(B_v,\, B_v). \tag{15}$$

Hence, system (13) can be rewritten as

$$\dot{y} = Ay + Gu + G_d d\,, \tag{16}$$

where $y = [y_r^T,\, y_v^T]^T$, $G = [0,\, I]^T$ and $G_d = [0,\, (B_v^{-1})^T]^T$. Similarly, the constraint (14) takes the form

$$\|C\, y_r(t)\|_\infty \leq 1, \tag{17}$$

where $C = WB_v$. Notice that, in the formulation (16)-(17), the $n$ double integrators have been decoupled, but the state constraints (17) are now coupled. In fact, while the feasible set for $x_r$ in (13) is a box, that of $y_r$ in (16) is a parallelotope.

For the systems (13) and (16), the minimum-fuel conditions (5)-(6) become

$$\begin{aligned} J_f(u^*) &= \sum_{j=1}^{n} J_f(u_j) = \|k\|_1 \\ u_j^*(t) &\in \{0, -\bar{k}_j\} \quad j = 1, \ldots, n\,, \end{aligned} \tag{18}$$

where $k = B_v^{-1} d$ and $\bar{k}_j = \text{sgn}(k_j)$. The minimum switching problem (9) can be generalized to the considered multivariable system, by suitably adapting the cost $J_s(u)$. Since we are interested in reducing as much as possible the number of input transitions per actuator, this amounts to minimize the maximum $J_s(u_i)$ over all inputs $u_i$, $i = 1, \ldots, n$. This corresponds to solving the problem

$$\begin{aligned} \min_{u} \ \max_{j} \quad & J_s(u_j) \\ \text{s.t.} \quad & (16), (17), (18). \end{aligned} \tag{19}$$

Problem (19) is hard to solve if all feasible solutions $y(t)$ are considered. Therefore, taking inspiration from the optimal solution (11) of the single-axis problem, we restrict our attention to solutions of the form

$$\begin{aligned} y_j(t) &= a_j\, f(\xi_j) \\ \xi_j &= t/p_j + \phi_j \\ a_j &= p_j^2\, \gamma_j \\ \gamma_j &= |k_j|\,(1 - |k_j|)/16 \quad j = 1, \ldots, n, \end{aligned} \tag{20}$$

where $f(\xi_j) \in [-1, 1]$ is given by (12) and the input signals turn out to be

$$u_j(t) = \begin{cases} -\bar{k}_j & \text{if} \ \ 0 \ \leq \text{mod}\ (\xi_j, 1) \leq |k_j| \\ 0 & \text{if} \ \ |k_j| < \text{mod}\ (\xi_j, 1) \leq \ 1. \end{cases} \tag{21}$$

The input signals $u_1, \ldots, u_n$ in (21) satisfy (18), hence they are fuel-optimal. Being these signals double-switch periodic, one has

$$J_s(u_j) = \frac{2}{p_j}. \tag{22}$$

Moreover, (17) is equivalent to

$$\max_i \ \max_t\ |s_i(t)| \leq 1, \tag{23}$$

where

$$s_i(t) = \sum_{j=1}^{n} c_{ij}\, y_j(t) \tag{24}$$

and the coefficients $c_{ij}$ are the entries of $C$. By enforcing (20) and replacing (17) by (23), problem (19) becomes

$$\begin{aligned} \min_{p,\,\phi} \quad & \max_j \ \frac{2}{p_j} \\ \text{s.t.} \quad & (20),\ (23),\ (24) \\ & 0 \leq \phi_j \leq 1 \\ & p \geq 0, \end{aligned} \tag{25}$$

where $p = [p_1, \ldots, p_n]$, $\phi = [\phi_1, \ldots, \phi_n]$. Notice that the solution of problem (25) does not change if all phases $\phi_i$ are shifted by the same quantity. Hence, without loss of

generality, in the sequel we will enforce $\phi_1 = 0$. So far, the dynamic optimization problem (19) has been converted into a static optimization problem, where the decision variables are $p$ and $\phi$. Note, however, that the problem is still difficult, being non-convex in the decision variables $p$ and $\phi$. Consequently, some simplifying assumptions will be made in order to obtain a sub-optimal solution.

In order to derive an upper bound to the solution of problem (25), we observe that

$$\max_t \mid s_i(t) \mid \leq \max_t \sum_{j=1}^{n} |c_{ij}| \, |y_j(t)| \leq \sum_{j=1}^{n} |c_{ij}| \, a_j, \quad (26)$$

and hence (23) can be enforced by imposing

$$|C| \, a \leq \mathbb{1}, \quad (27)$$

where $|C| = \{|c_{ij}|\}$, $a = [a_1, \ldots, a_n]^T$ and $\mathbb{1}$ denotes a column vector whose components are all equal to one. From (20), it follows that

$$p_j = \sqrt{a_j/\gamma_j}. \quad (28)$$

By replacing (23) with (27) and substituting (28) in (22), problem (25) boils down to

$$\begin{array}{ll} \min\limits_{a} & \max\limits_{j} \; 2\sqrt{\dfrac{\gamma_j}{a_j}} \\ \text{s.t.} & |C|a \leq \mathbb{1} \\ & a \geq 0. \end{array} \quad (29)$$

By (26), the solution of (29) is an upper bound to that of (25). It turns out that problem (29) can be solved analytically, as stated by the following theorem.

*Theorem 1:* A global minimum of problem (29) is attained at

$$a^* = \frac{1}{\|Q\|_\infty} \Gamma \, \mathbb{1} \quad (30)$$

where $\Gamma = \text{diag}(\gamma)$, $Q = |C|\Gamma$, and $\|\cdot\|$ denotes the matrix infinity norm.

*Proof:* Let $x = \Gamma^{-1} a$. Then, problem (29) can be rewritten as

$$\begin{array}{ll} \min\limits_{\beta, x} & \beta \\ \text{s.t.} & \dfrac{2}{\sqrt{x_j}} \leq \beta, \quad j = 1, \ldots, n \\ & Qx \leq \mathbb{1} \\ & x \geq 0 \end{array} \quad (31)$$

The statement of the theorem is proven if $x^* = \frac{1}{\|Q\|_\infty}\mathbb{1}$, $\beta^* = 2\sqrt{\|Q\|_\infty}$ is a global minimum for problem (31). Let $\hat{x}$, $\hat{\beta}$ be a feasible solution of (31). From feasibility, we get

$$\hat{x}_j \geq \frac{4}{\hat{\beta}^2}, \quad \forall j = 1, \ldots, n$$

and, being $q_{ij} \geq 0$, $\forall i, j$,

$$1 \geq \sum_{j=1}^{n} q_{ij} \hat{x}_j \geq \frac{4}{\hat{\beta}^2} \sum_{j=1}^{n} q_{ij}, \quad \forall i = 1, \ldots n.$$

Hence,

$$\hat{\beta} \geq 2\sqrt{\max_{i=1,\ldots,n} \sum_{j=1}^{n} q_{ij}} = \beta^*$$

which concludes the proof. ■

*Remark 1:* Since by (30) all the entries of $\Gamma^{-1} a^*$ are equal, it follows from (28) that

$$p_1^* = p_2^* = \ldots = p_n^* = \frac{1}{\sqrt{\|Q\|_\infty}}. \quad (32)$$

Similarly to the single-axis case, the optimal input $u_j^*$ is pulse-width modulated with period $p_j^*$ and duty cycle $|k_j|$.

In the relaxation (29) of problem (25), the additional degrees of freedom provided by the decision variables $\phi$ have not been exploited. In order to find a less conservative relaxation, we enforce directly the property (32) into the original problem (25). This leads to the new relaxed problem

$$\begin{array}{ll} \max\limits_{p, \, \phi} & \dfrac{p_1}{2} \\ \text{s.t.} & \text{(20), (23), (24)} \\ & 0 \leq \phi_j \leq 1 \\ & p_1 = p_2 = \ldots = p_n \geq 0, \end{array} \quad (33)$$

where $\phi_1 = 0$. Due to (32) and the fact that (23) is less restrictive than (27), the solution of problem (33) is a lower bound to that of (29), while still being an upper bound to that of (25). By exploiting (20) and (24), we rewrite the constraint (23) as

$$p_1^2 \, \sigma(\phi) \leq 1 \quad (34)$$

where

$$\sigma(\phi) = \max_i \max_{0 \leq t \leq p_1} \Big| \sum_{j=1}^{n} c_{ij} \, \gamma_j f(t/p_1 + \phi_j) \Big|. \quad (35)$$

Notice that $\sigma(\phi)$ in (35) does not depend on the actual value of the period $p_1$, because the peak values of the sums of the $p_1$-periodic functions $f(t/p_1 + \phi_j)$, evaluated over the period, are independent from the period itself. Hence, the global maximum of problem (33) is attained at

$$p_1^* = \frac{1}{\sqrt{\sigma(\phi^*)}}, \quad (36)$$

where

$$\sigma(\phi^*) = \min_{\phi} \; \sigma(\phi). \quad (37)$$

According to (21), the optimal input $u_j^*$ is pulse-width modulated with period $p_j^* = p_1^*$, duty cycle $|k_j|$ and phases $\phi_1 = 0$ for $j = 1$, and $\phi_j^*$ for $j = 2, \ldots, n$.

The unconstrained problem (37) is essentially a crest factor minimization problem, which is known to be a hard optimization problem, being $\sigma(\phi)$ a non convex function (see [17] for a study of the crest factor problem in the sinusoidal case). Nevertheless, for low dimensional cases, such as $n = 2$ or $n = 3$, which are of practical interest in several applications, a global minimizer of (37) can be found by numeric search over the free phases $\phi_j$. The benefits of this approach over the solution provided by Theorem 1 are demonstrated on two numerical examples, in the next section.

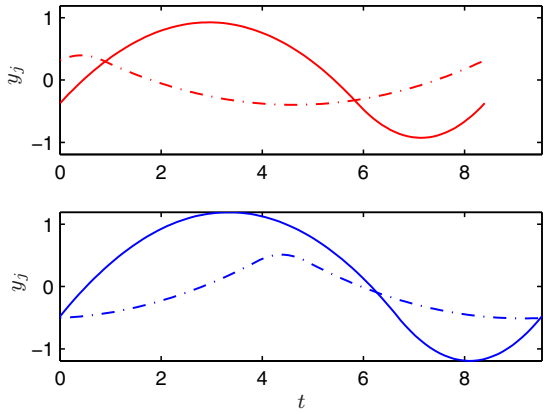


Fig. 4. Trajectories $y_1(t)$ (solid) and $y_2(t)$ (dash-dotted) from the solution to (29) (top) and (33) (bottom).

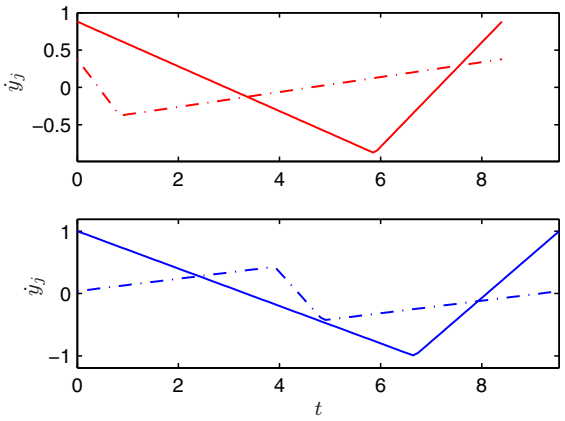


Fig. 5. Velocities $\dot{y}_1(t)$ (solid) and $\dot{y}_2(t)$ (dash-dotted) from the solution to (29) (top) and (33) (bottom).

## IV. Numerical examples

In this section, two numerical examples are presented. We will refer directly to system (16), the interpretation in terms of system (13) being straightforward by means of (15).

### A. Two-axis example

Let $n = 2$, $W = I$ in (14) and

$$B_v = \begin{bmatrix} \cos(\pi/3) & \sin(\pi/3) \\ -\sin(\pi/3) & \cos(\pi/3) \end{bmatrix}$$

in (15). Then, $C = B_v$ in (17). Moreover, assume that $k = [0.7,\, 0.1]^T$ . In the following, the solutions to (29) and (33) are compared. According to (30), the solution to (29) is given by $a^* = [0.9257,\, 0.3967]^T$. From (32), it follows that $p_1^* = p_2^* = 8.4$ and hence the maximum switching frequency is $J_s(u^*) = 2/p_1^* = 0.238$.

In order to exploit the additional degrees of freedom provided by $\phi$, problem (33) is solved using (36) and (37) with $\phi_1 = 0$, where the solution of (37) is found numerically through a one-dimensional search over $\phi_2$. The solution is $p_1^* = p_2^* = 9.53$ and $\phi_2^* = 0.59$, which gives $J_s(u^*) = 2/p_1^* = 0.21$. Hence, the optimal cost of (33) is lower than the optimal cost of (29) by approximately 12%.

The trajectories $y_1(t)$, $y_2(t)$ of system (16) are obtained by substituting the solutions $p^*$ and $\phi^*$ in (20), for both approaches. Since the solution of (29) holds for any $\phi$, without loss of generality one can assume $\phi_1^* = \phi_2^* = 0$ in the first approach. The resulting trajectories are reported in Fig. 4 on a single period. The corresponding velocities are reported in Fig. 5. The same trajectories are reported in the $y_1\, y_2$ plane in Fig. 6, together with the set defined by (17) and the box $|y_i| \le a_i^*$. It can be clearly seen that the control requirements (17) are met in both cases. However, the trajectories satisfying (30) are constrained to lie inside a smaller region, which, being the period proportional to the square root of the oscillation amplitude, translates into a higher frequency of input transitions.

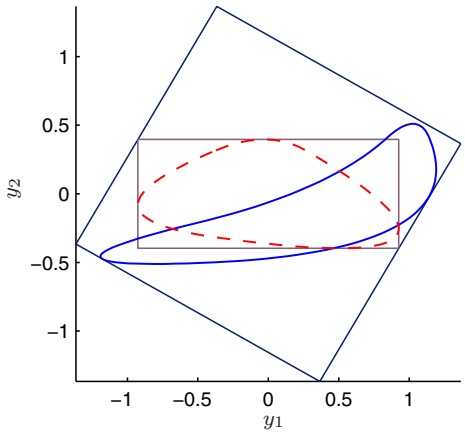


Fig. 6. Trajectories in the $y_1, y_2$ plane of the solutions to (29) (dashed) and (33) (solid), with constraints (17) (outer parallelogram) and $|y_i| \le a_i^*$ (inner box).

### B. Three-axis example

In spacecraft attitude control problems with on/off actuators, the model describing the three-dimensional rotational dynamics of the attitude error with respect to the principal axes of inertia of the spacecraft is typically approximated by (13) [14]. Since the control accuracy requirements are commonly specified as the maximum acceptable angular error about the principal axes, one can assume that $W = I$ in (14). In order to maximize the torque generated by the actuators and meet constraints coming from the spacecraft layout, it is often the case that thruster configurations not aligned to the principal axes are adopted, which implies that $B_v$ is not diagonal in (15). In this example, we consider

$$B_v = \frac{1}{1.393} \begin{bmatrix} 0.9 & -0.8 & 0.7 \\ 0.7 & 0.9 & -0.8 \\ -0.8 & 0.7 & 0.9 \end{bmatrix}$$

Moreover, let $k = [0.1,\, 0.5,\, -0.2]^T$.

The solution to (29) is $a^* = [0.301\,, 0.837,\, 0.536]^T$, which corresponds to the period $p_1^* = p_2^* = p_3^* = 7.32$ and the optimal cost $J_s(u^*) = 0.273$. In order to solve (33) through

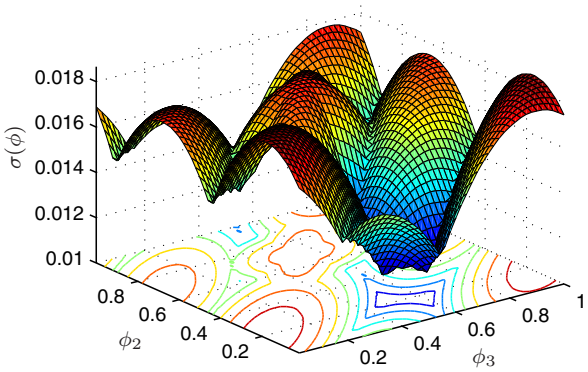


Fig. 7. Value of $\sigma(\phi)$ as a function of $\phi_2$ and $\phi_3$.

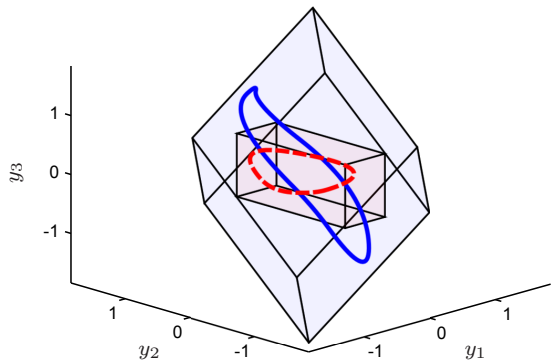


Fig. 8. Trajectories of the solution to (29) (dashed) and (33) (solid), together with constraints (17) (outer parallelotope) and $|y_i| \leq \alpha_i^*$ (inner box).

(36), one has to search the 2-dimensional parameter space $\phi_2, \phi_3$ for a global minimizer of (37). Notice that $\sigma(\phi)$ in (36) is a non-convex function of the decision variables $\phi$, as can be observed in Fig. 7. The solution to (33) is $p_1^* = p_2^* = p_3^* = 9.5$, $\phi_2^* = 0.17$ and $\phi_3^* = 0.6$, corresponding to the optimal cost $J_s(u^*) = 0.21$. As expected, when $\phi$ is optimized, the pulse modulation scheme requires a lower switching frequency, while the average fuel consumption $J_f(u^*) = \|k\|_1 = 0.8$ is the same for both solutions, by construction. The optimal cost of (33) is lower than the optimal cost of (29) by approximately 23%, which is a significant performance improvement for the considered application. The three-dimensional plot of the trajectories $y_1(t)$, $y_2(t)$ and $y_3(t)$ is reported in Fig. 8, where it can be seen that the control accuracy requirements (represented by the 3-dimensional parallelotope) are satisfied.

## V. Conclusions

The problem of finding the fuel/switch-optimal limit cycles for coupled double integrators driven by switching inputs, in the presence of a constant disturbance term, has been addressed. Focusing on the class of periodic single-axis trajectories featuring the same period, the problem is cast as a static optimization problem. The limit cycles resulting from the numerical solution of such a problem turn out to perform significantly better in terms of number of input transitions than an analytic suboptimal solution neglecting the possibility of tuning the limit cycle phases. However, an effective procedure to find a numerical solution for high dimensional systems still needs a deeper investigation.

The opportunity of considering a larger class of periodic single-axis trajectories, having commensurable (possibly different) periods, is under investigation. Moreover, an underlying assumption of this work is that in the multivariable case the switch-optimal trajectories are still unimodal limit cycles, as it occurs in the single-axis case. The question whether more complex oscillations can actually provide a lower switching frequency is still unanswered.

## References


[1] Tsypkin, Y. Z., *Relay Control Systems*, Cambridge University Press, UK, 1984.

[2] Åström, K. J., "Oscillations in systems with relay feedback," *Adaptive Control, Filtering, and Signal Processing*, 1995, pp. 1–25.

[3] Gonçalves, J. M., Megretski, A., and Dahleh, M. A., "Global stability of relay feedback systems," *IEEE Transactions on Automatic Control*, Vol. 46, No. 4, 2001, pp. 550–562.

[4] Nugent, S. and Kavanagh, R., "Self and forced oscillations in multivariable relay control systems," *Automatica*, Vol. 5, No. 4, 1969, pp. 519–527.

[5] Loh, A. and Vasnani, V., "Necessary conditions for limit cycles in multiloop relay systems," *IEE Proceedings - Control Theory and Applications*, Vol. 141, No. 3, 1994, pp. 163–168.

[6] Boiko, I., Pisano, A., and Usai, E., "Frequency-domain analysis of self-excited oscillations for a class of multivariable relay systems," *European Control Conference*, 2013, pp. 4287–4292.

[7] Gonçalves, J. M., "Regions of stability for limit cycle oscillations in piecewise linear systems," *IEEE Transactions on Automatic Control*, Vol. 50, No. 11, 2005, pp. 1877–1882.

[8] Flieller, D., Riedinger, P., and Louis, J.-P., "Computation and stability of limit cycles in hybrid systems," *Nonlinear Analysis: Theory, Methods & Applications*, Vol. 64, No. 2, 2006, pp. 352–367.

[9] Patino, D., Riedinger, P., and Iung, C., "Practical optimal state feedback control law for continuous-time switched affine systems with cyclic steady state," *International Journal of Control*, Vol. 82, No. 7, 2009, pp. 1357–1376.

[10] Ding, X., Wardi, Y., Taylor, D., and Egerstedt, M., "Optimization of switched-mode systems with switching costs," *American Control Conference*, 2008, pp. 3965–3970.

[11] Deng, H., Larsen, L., Stoustrup, J., and Rasmussen, H., "Control of systems with costs related to switching: applications to air-condition systems," *Control Applications (CCA) & Intelligent Control (ISIC)*, 2009, pp. 554–559.

[12] Solberg, B., Andersen, P., Maciejowski, J. M., and Stoustrup, J., "Optimal switching control of burner setting for a compact marine boiler design," *Control Engineering Practice*, Vol. 18, No. 6, 2010, pp. 665–675.

[13] Leomanni, M., Garulli, A., Giannitrapani, A., and Scortecci, F., "An MPC-based attitude control system for all-electric spacecraft with on/off actuators," *52nd IEEE Conference on Decision and Control*, 2013, pp. 4853–4858.

[14] Kaplan, M. H., *Modern spacecraft dynamics and control*, John Wiley and Sons, New York, 1976.

[15] Hanawa, Y., *Fuel efficient attitude control of spacecraft*, Ph.D. thesis, Massachusetts Institute of Technology, 1979.

[16] Cervin, A. and Åström, K. J., "On limit cycles in event-based control systems," *46th IEEE Conference on Decision and Control*, 2007, pp. 3190–3195.

[17] Boyd, S., "Multitone signals with low crest factor," *IEEE Transactions on Circuits and Systems*, Vol. 33, No. 10, 1986, pp. 1018–1022.